2002

Design Improvement Of A Compressor Bearing Using An Elastohydrodynamic Lubrication Model

M. Duyar
Arcelik A.S.

Z. Dursunkaya
Middle East Technical University

DESIGN IMPROVEMENT OF A COMPRESSOR BEARING USING AN ELASTOHYDRODYNAMIC LUBRICATION MODEL

***Mustafa DUYAR;** Product Development Engineer, Arcelik A.S. Compressor Plant
26540 Eskisehir Turkey; Phone: +90 222 236 0635; Fax: +90 222 236 0344
e-mail: mustafa.duyar@arcelik.com

Zafer DURSUNKAYA; Associate Professor, Department of Mechanical Engineering,
Middle East Technical University; 06531 Ankara Turkey
Phone: +90 312 210 5232 and +90 312 210 2504; Fax: +90 312 210 1110
e-mail: refaz@metu.edu.tr

ABSTRACT

Efficiency and reliability of reciprocating hermetic compressors are of increasing interest, due to stricter energy consumption regulations and customer demands. Optimization of bearing design is particularly important, since one of the main contributors to power loss materializes at the compressor bearings. After prolonged operation, there could be scoring, sometimes scuffing or seizure at the piston pin bearing, which results in a decrease in the efficiency and reliability of the compressor. In this study a model of elastohydrodynamic lubrication of reciprocating compressor wristpin bearing was developed along with the simulation of the slider-crank mechanism of motion. Slider-crank dynamics, wristpin elastohydrodynamic and boundary lubrication, and elastic deformations are simultaneously solved in the computation. Deformations are calculated using the wristpin compliance matrix derived from a finite element model of the wristpin. The methodology was used to understand the physics of lubrication of the small end bearing, particularly the necessity of using an elastic model *versus* a rigid one. The design parameters were altered to reach a superior design in terms of reduced boundary lubrication and projected wear.

NOMENCLATURE

A	: Coefficient matrix of pressures
a_4	: Piston acceleration
$\mathbf{C}$	: Compliance matrix
e	: Eccentricity
F_{gas}	: Gas force on piston
F_{34}	: Force on wristpin
h	: Clearance array
h_{dyn}	: Clearance due to geometry
L	: Bearing axial length
m_{3b}	: Connecting rod equivalent mass
m_4	: Piston mass
P	: Oil pressure
P_c	: Contact pressure
P_{sc}	: Suction pressure
R	: Wrist-pin radius
t	: Time
z	: Axial coordinate on the bearing
α	: Crank angle
β	: Connecting rod angle
δ	: Radial deformation array
θ	: Angular coordinate on the bearing
μ	: Viscosity
ϕ	: Attitude angle
ω	: Connecting rod rotational speed

INTRODUCTION

Analysis of compressor bearing lubrication is important for design engineers to reduce power loss while maintaining reliability. Among compressor bearings, connecting rod small end bearing requires careful attention, due to the complex dynamics and high loads applied on the bearing. Wristpin bearing, which is a dynamically loaded journal bearing, carries loads that vary in magnitude and direction. A schematic diagram of a dynamically loaded journal bearing is shown in Figure 1. The angular velocities of journal and sleeve vary in direction and magnitude. The radial and tangential velocities, $\dot{e}$ and $e\dot{\phi}$, are depicted for a specific position of load, sleeve and journal. The pressure distribution inside the bearing is seen to increase gradually: starting at $\theta=\theta_1$, reaching the maximum value at $\theta=\theta_{pmax}$, beyond which the pressure drops to zero at $\theta=\theta_2$. The variation in load alters

journal center velocity and causes fluctuation in the angular position of start (θ_1) and end (θ_2) of the pressure distribution curve, resulting in a varying minimum film thickness and corresponding variation in the peak pressure. The interacting surfaces of the bearing and wristpin are, therefore, subjected to fluctuating stress, rendering fatigue strength an important consideration in the selection of material. Therefore, it is necessary to evaluate the trend of minimum film thickness to prevent bearing wear and maximum film pressure to avoid fatigue for reliable bearing performance.

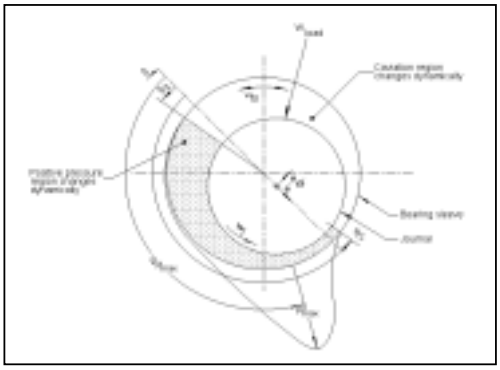

Figure 1. Schematic diagram of dynamically loaded journal bearing

The elastohydrodynamic lubrication (EHL) approach is given by Dowson and Higginson, [1]; Hamrock and Dowson, [2]; and Gohar [3], and it accurately predicts the profile and thickness of the lubricating film. The use of EHL approach in the design has, therefore, brought about a large improvement in working performance and durability of bearings. In this lubrication regime hydrodynamic pressures are sufficiently high that a significant elastic deformation of the interacting surfaces are caused. The use of EHL approach shows that the film thickness is slightly influenced by the elastic moduli of surfaces. The EHL analysis of connecting rods has been of considerable interest in the last two decades. Implementations of improved fixed point EHL-iteration schemes were presented by LaBouff and Booker [4] as well as by Fantino and Frene [5]. Oh and Goenka [6] presented a stable and fast Newton-Raphson scheme and a solution. Van der Tempel et al. [7, 8] combined Newton-Raphson and inverse hydrodynamic methods, an approach that is very well suited for highly compliant bearing structures. Kumar et al. [9] introduced modal reduction techniques for faster solutions in the context of quasi-static deformation analysis, an attribute that holds for all the above references. Dursunkaya et al. [10] solved the EHL problem of a piston in the context of the analysis of secondary dynamics of piston components. In this study a similar approach is used for the analysis of the EHL in the solution of the wristpin-small end bearing. Slider-crank dynamics is solved to provide dynamics data for the lubrication problem, where, wristpin elastohydrodynamic and boundary lubrication, and elastic deformations are simultaneously solved. The deformations are calculated using the wristpin compliance matrix derived from a finite element model of the wristpin.

MODELING AND SOLUTION

Slider-Crank Dynamics:

The slider-crank mechanism must be analyzed to obtain the kinetics and kinematics. The rotational speed of the connecting rod relative to the wristpin was solved for the given crank speed. The axial and lateral force balances on the pin were written. The forces on the wristpin are,

$$F_{x_{34}} = m_4 \cdot a_4 + F_{gas} \qquad (1a)$$

$$F_{y_{34}} = -\left\{\left(m_{3b} + m_4\right) \cdot a_4 + F_{gas}\right\} \cdot \tan\beta \qquad (1b)$$

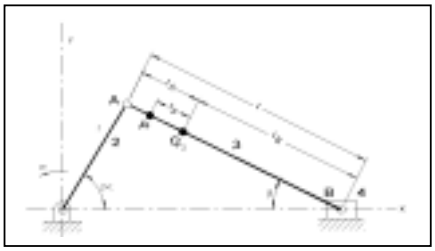

Figure 2. Slider-Crank Mechanism

The resulting equations are solved to give the relative position of the sleeve in the journal.

Wristpin Elastohydrodynamic Lubrication:

The equations governing the wristpin EHL problem are the Reynolds equation for the pressure distribution and the elasticity relationships for wristpin deformation. The following form of the Reynolds equation is used:

$$\frac{\partial}{\partial z}\left(h^3\frac{\partial P}{\partial z}\right)+\frac{1}{R^2}\frac{\partial}{\partial \theta}\left(h^3\frac{\partial P}{\partial \theta}\right)=-6\mu\omega R\frac{\partial h}{\partial \theta}+12\mu\frac{\partial h}{\partial t} \qquad (2)$$

The film thickness h includes the effect of connecting rod motions, bearing clearance and elastic deformation. Only radial deformations on bearing surface of the wristpin are considered. Other (axial, tangential) deformations are comparatively small and do not affect local film thickness. The elastic relationship relating radial deformations on these surfaces to the applied pressure is given by,

$$\delta(z,\theta,t)=\mathbf{C}\cdot(P+P_c) \qquad (3)$$

The compliance matrix includes the effect of the area and, therefore, the nodal radial deformations are linearly related to nodal pressures. The distributions of wristpin elastic deformation δ and the film thickness h are related to each other by,

$$h(z,\theta,t)=h_{dyn}(z,\theta,t)+\delta(z,\theta,t) \qquad (4)$$

The pressure inside the hermetically sealed shell is equal to suction pressure, resulting in the following boundary conditions in the axial direction,

$$P=P_{sc},\ z=0,L \qquad (5)$$

In the cavitating region, Half Sommerfeld condition is assumed to be valid, therefore,

$$P=0,\ \text{if}\ P<0 \qquad (6)$$

For bearing surfaces in close proximity, a model for contact pressures between two nominally flat surfaces (Greenwood and Trip, [11]) is used. The model has a statistical representation of surface roughness, which uses three roughness parameters, and is used to calculate the effective asperity contact pressure at each point of the EHL mesh.

For the solution of the problem the approach explained used in [10] was used. The Reynolds equation was discretized, and the resulting set of equations was solved iteratively till the pressures and deformations converged. This loop was further embedded in another iterative scheme, where the force balance on the pin was satisfied. The solution was advanced in time. The entire problem is solved typically for 5-7 cycles, after which results are cyclically repeating. Note that for a rigid wristpin with no elastic deformations, the Reynolds equation can be solved directly for the film thickness resulting from the position of the connecting rod small end relative to wristpin.

Compliance Matrix, FE model:

The bearing surface of the wristpin compliance matrix used in the EHL calculation is extracted using standard FE codes, from an FE model of the wristpin as shown in Figure 3. Connecting rod was considered as rigid and wristpin was considered as elastic in the computation. The FE code is used to obtain –*via* a substructure analysis– the bearing surface of wristpin stiffness matrix; a pre-processing program inverts the stiffness matrix to obtain the compliance matrix to be used in the EHL code. The stiffness/compliance matrices are generated for the radial degrees of freedom on the surface of wristpin. In specifying the elastic problem, the nodes contacting the piston pin hole are restrained.

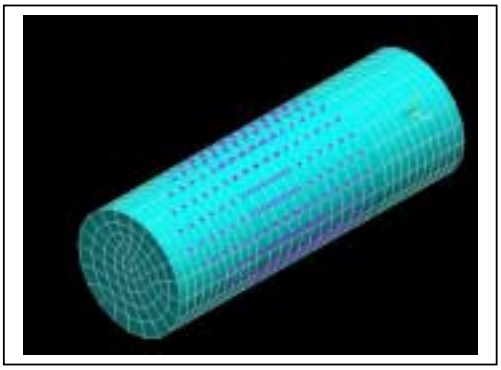

Figure 3. FE Model of Wristpin

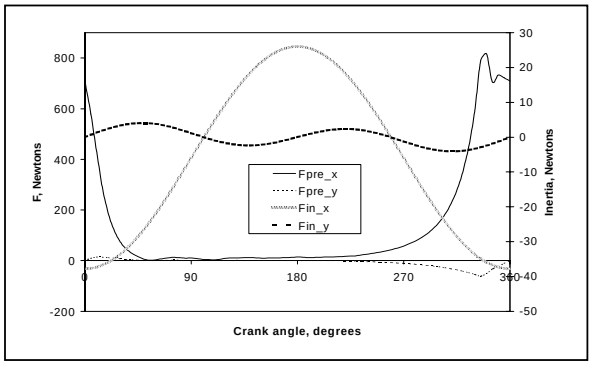

Figure 4. Pressure Force and Inertia at the Wristpin

RESULTS AND DISCUSSION

The predictions of the current approach were compared to a commercially available finite difference computer code. The physical dimensions and pressure data of the compressor running at ASHREA conditions, pertaining to a production Arcelik TE165 compressor were used in the study. Simulations were run till cyclic convergence was achieved, typically 5 cycles. When the lubricant viscosity was increased number of cycles to reach convergence increased to 7. Figure 4 shows the compression pressure force and inertia at the wristpin.

Figures 5a, 5b and 5c show the predictions of the current study using a rigid, elastohydrodynamic analysis and the rigid analysis of the commercial code. The minimum film thickness and maximum deformations during a thermodynamic cycle are given in Figure 5a. The predictions using the rigid assumption of the commercial code and the current study match well. There is negligible difference between the minimum film thickness predictions of the current study using an elastic and rigid approach. The deformations of the wristpin are of the order of 0.5μm, which, although small in magnitude, amount to approximately 10-15% of the clearance. The necessity of an elastic modeling, however, can be appreciated when the forces along the axial direction on the wristpin are examined. Figures 5b and 5c show the hydrodynamic and boundary contact forces acting on the pin for the rigid and elastohydrodynamic simulations using the current code and the rigid simulations of the commercially available code. The rigid simulations predict boundary contact forces of maximum 45 Newtons, whereas the elastohydrodynamic simulation results in boundary forces of maximum only 40 Newtons. This is due to the fact that, despite the deformation levels are low, the wristpin deforms under the effect of hydrodynamic and boundary pressures, conforming to the shape and hence reducing the boundary contact. This is especially important in the prediction of wear, which is a direct result of metal-to-metal contact. However, it is better to analyze the comparative change in the contact forces, rather than their magnitudes. The magnitudes depend upon the parameters used in [11] and are sensitive to physical data that cannot be measured easily, such as the radius of curvature of asperities, and the asperity density per unit area. Therefore, the model needs to be carefully used for a particular application, if realistic magnitudes for asperity contact forces are needed. In this study, only the effect of design parameters on the boundary contact forces, and its trend were analyzed, rather than the absolute magnitudes of these forces. There is an observed difference between the rigid solution of the present study and the commercial code in boundary contact forces in the *y*-direction. The commercial code has a discontinuity around 270° crank angle, which cannot be accounted for.

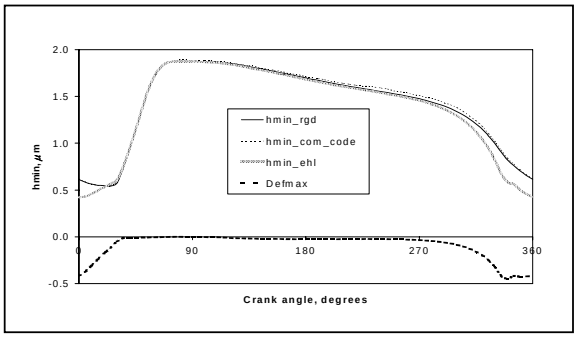

Figure 5a. Minimum Clearance and Maximum Deformation

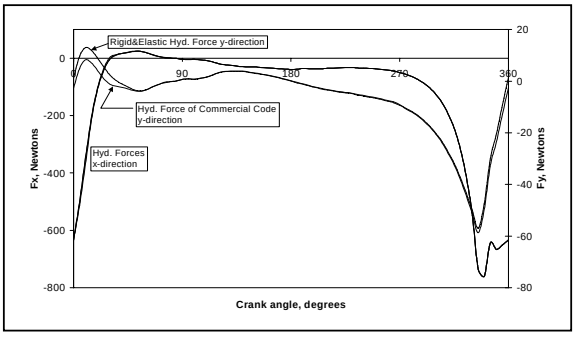

Figure 5b. Hydrodynamic Forces

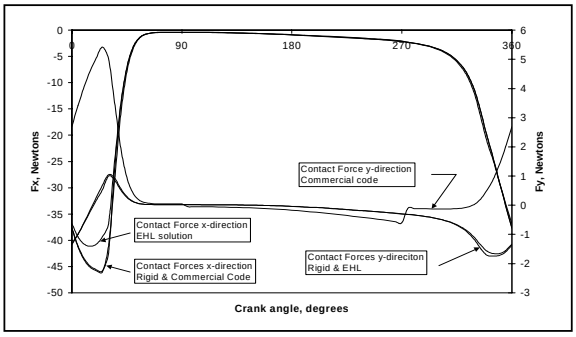

Figure 5c. Boundary Contact Forces

I. Effect of Viscosity Variation:

The effect of lubricant temperature –hence viscosity– on the performance was studied. In case of the baseline simulation, the fluid was at 100°C, and the other cases were exercised for fluid at 75°C, 50°C and 25°C. Figure 6a shows the effect of viscosity variation on the orbital motion inside the bearing and the radial deformation of the pin. It can be seen that with a decrease in temperature, and corresponding increase in lubricant viscosity, the motion of the pin inside the sleeve slows down. With reduced viscosity, the pin moves inside the sleeve under the effect of the cyclically varying load, and an increase in viscosity keeps the pin at a relatively less varying distance from the sleeve. As far as the boundary contact and the resulting wear are concerned, this has two contradictory consequences. The pin comes to a closer proximity of the sleeve near TDC, when the load is at a maximum when the viscosity is low, thus increasing the boundary contact. On the other hand, elsewhere during the cycle, the pin assumes a more centered position diminishing boundary contact. When the boundary forces in the axial direction are viewed in Figure 6b, this effect can be seen. The baseline case results in large boundary forces near 0°, TDC but elsewhere the boundary forces are small. With an increased viscosity, the contact phenomenon near TDC eases, but at other locations the magnitude of boundary forces are more elevated compared to the baseline case. The effect of this on wear needs to be further investigated. The change in lubricant viscosity did not affect the deformations considerably.

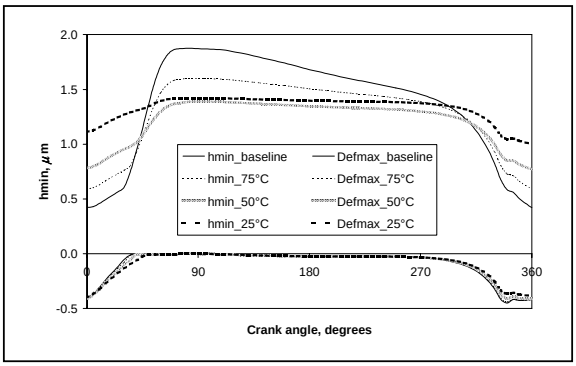

Figure 6a. Minimum Clearance and Maximum Deformation

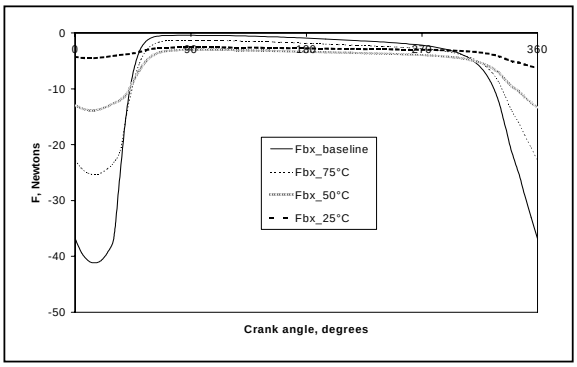

Figure 6b. Boundary Contact Forces

II. Effect of Nominal Clearance:

To study the effect of bearing clearance on the performance, simulations were carried out for various conrod-pin nominal radial clearances. For the baseline case, the radial clearance was 4μm, and the other cases were run for clearances of 3.5 μm, 5 μm, 6μm, 7μm, and 8μm. Figure 7a shows the effect of nominal clearance on the minimum film thickness and the radial deformation of the pin. It can be seen that with an increase in clearance, the motion of the pin inside the journal is accelerated. With reduced clearance, the pin moves inside the sleeve under the effect of the cyclically varying load, and a decrease in clearance keeps the pin at a relatively less varying distance from the sleeve. As far as the boundary contact and the resulting wear are concerned, two contradictory consequences occur, similar to the viscosity sweep case. Figure 7b shows that a reduction in nominal clearance reduces the boundary contact force occurring near the TDC, however, elsewhere in the cycle there occurs a prolonged but diminished boundary contact. An increase in the nominal clearance has just the opposite effect. The overall effect of the nominal clearance on wear, therefore, needs additional study. The clearance alteration did not affect the deformations.

III. Effect of Pin Material:

Engineering materials, which could be considered as an alternative to the currently used (baseline) wristpin material, were investigated without any detailed consideration of strength. Aluminum alloy, bronze and titanium material properties were used in the simulation. The results are given in Figures 8a and 8b. The aluminum alloy has the minimum elastic modulus among the materials and this case resulted in the best conformity of the conrod and pin, resulting in maximum deformations. Baseline material is stiffer than the others; therefore deformations were smaller. Although the minimum film thickness of aluminum was smallest of the four, due to

larger deformations, it conformed better to the shape of the journal and a reduction in boundary contact force was realized throughout the cycle.

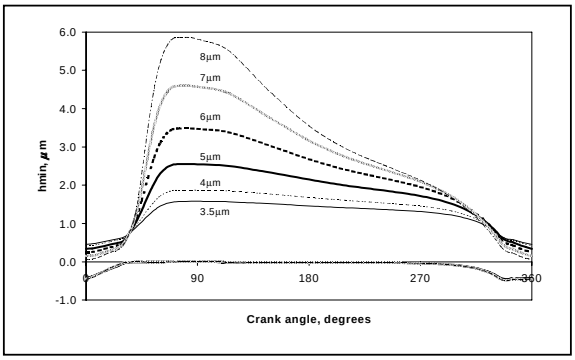

Figure 7a. Minimum Clearance and Maximum Deformation

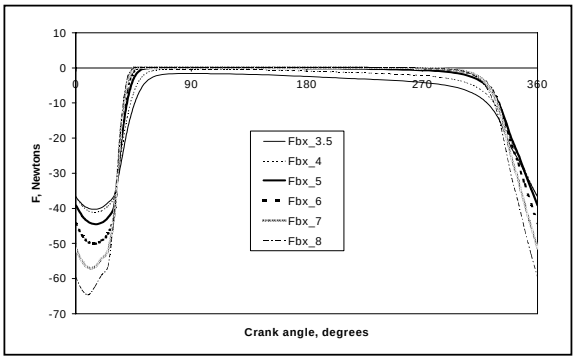

Figure 7b. Boundary Contact Forces

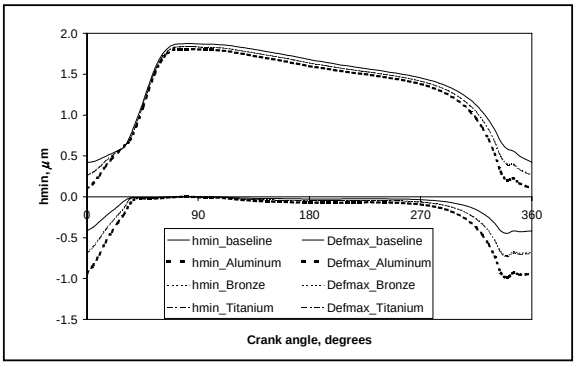

Figure 8a. Minimum Clearance and Maximum Deformation

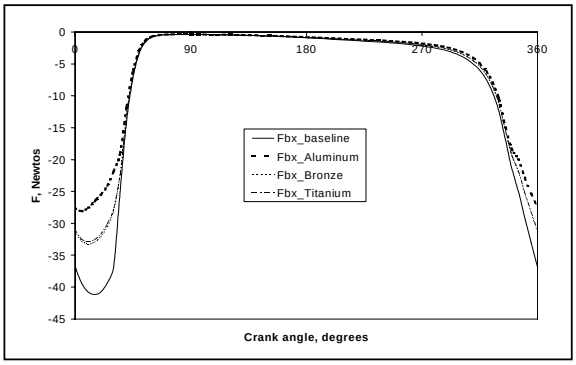

Figure 8b. Boundary Contact Forces

IV. Effect of Bearing Diameter:

The pin diameter affects the bearing performance, due to the fact that an increase in diameter increases the bearing area. For the baseline case the wristpin is 7.9324mm in diameter. Simulations were performed by increasing the baseline value by 10% and 20%, resulting in an increase in the hydrodynamic pressure acting area. The results are given in Figures 9a and 9b. The results showed that increasing the bearing diameter increased the minimum film thickness and also resulted in up to 20% reduction in maximum boundary contact forces.

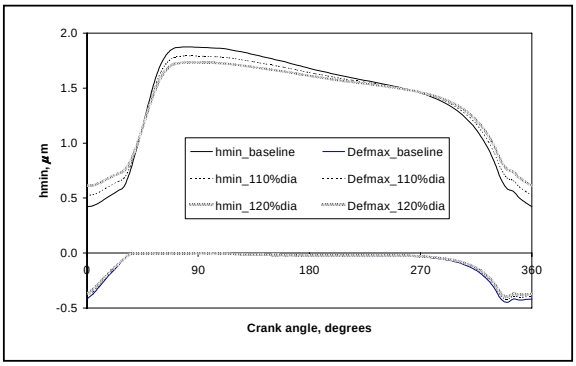

Figure 9a. Minimum Clearance and Maximum Deformation

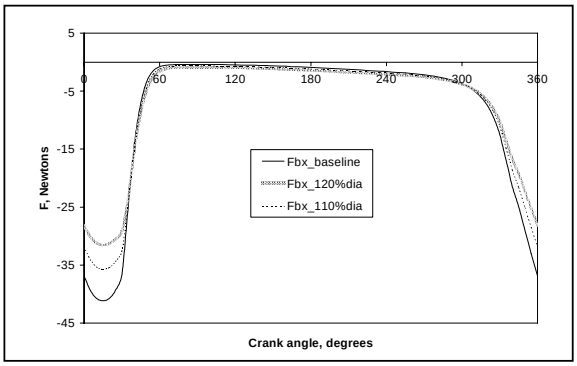

Figure 9b. Boundary Contact Forces

V. Effect of Bearing Length:

A change in bearing length directly affects the bearing performance. In an existing design, however, such a change may not be feasible. Nevertheless, the effect of wristpin bearing length on the performance was studied. In case of the baseline simulation, wristpin-bearing length is 8mm, two other cases were exercised, where the length is increased to 10mm and 16mm. Increasing the length to 10mm is practically possible, however, due to piston geometry of the design in question, using a 16mm bearing length not feasible. Using longer bearings increased the bearing area, as a result the hydrodynamic pressure acting area, minimum clearances around TDC increased, resulting in a decrease in boundary contact force, as can be seen from Figures 10a and 10b.

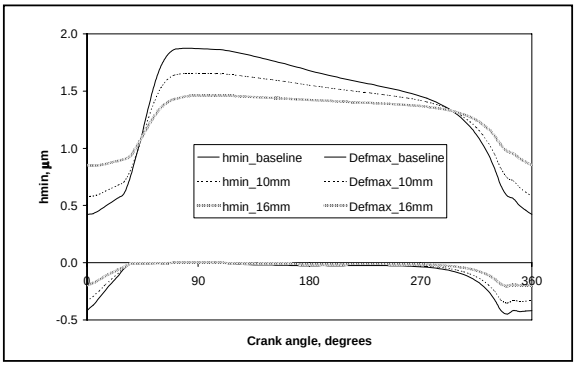

Figure 10a. Minimum Clearance and Maximum Deformation

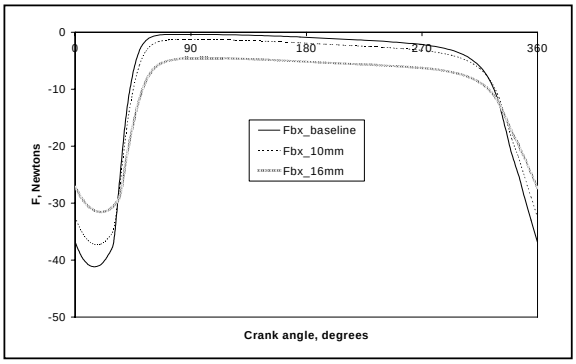

Figure 10b. Boundary Contact Forces

VI. Optimization:

The results of the previous parametric runs were analyzed to reach an "optimum" solution, with the aim of a reduction of boundary contact and wear. The term "optimum" is used in the sense that, a formal approach to finding an optimum design was not sought, but an overall analysis of the above results were made to reach at a set of parameters to result in a comparatively better solution. The results presented in Figures 11a and 11b show the minimum film thickness, pin deformation and boundary forces for the baseline case, and the three optimized cases. One used the viscosity at 25°C, a clearance of 4μm, an aluminum wristpin 20% larger diameter and a 16mm bearing length. As shown in Figure 11a, minimum clearance around TDC was increased from 0.5μm to nearly 2μm. Figure 11b shows that, boundary contact force for this case was almost zero all through the thermodynamic cycle. It is practically not possible to use a 16mm bearing length and 25°C lubricant temperature at the wristpin, therefore two more cases were run. In one case, keeping all other parameters the same a 75°C lubricant temperature was used. In the other case only the bearing length was reduced to 8mm. Increasing lubricant temperature to 75°C resulted in a considerable increase in boundary contact force. Therefore, it was concluded that the temperature of the lubricant at wristpin should be lowered. Using 8mm bearing length, instead of 16mm, did not alter the boundary contact force considerably, and deemed possible.

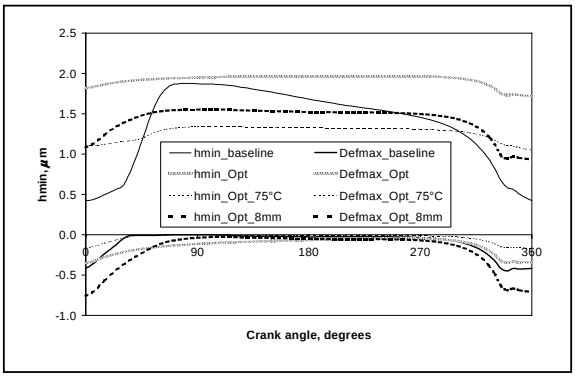

Figure 11a. Minimum Clearance and Maximum Deformation

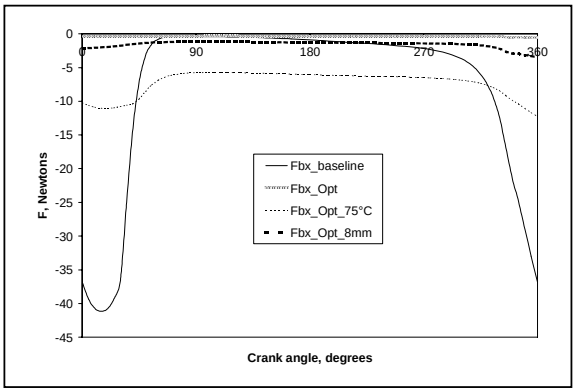

Figure 11b. Boundary Contact Forces

CONCLUSION

For an existing design, the parameters that can be altered and also govern the lubrication phenomenon in the pin bearing of a compressor are limited in number. Therefore, in order to suggest design alterations for improving the performance of the bearing, a detailed study of the effect of change on the performance is necessary.

In this study, the design parameters that can be changed without a major change in the design of the compressor were studied to understand the nature of the boundary lubrication and reduction in wear. To this end the effect of lowering the lubricant temperature, increasing the journal diameter, using a more conforming material to enhance conformance, changing the bearing length and clearance were investigated. It was concluded that using a more conforming bearing material and cooling the lubricant to increase its viscosity would result in a superior design. It was also seen that a rigid approach could not be used in this study. It should also be noted that an analysis that accounts for the elastic behavior of the connecting rod would result in a more realistic simulation of the underlying physical phenomena.

REFERENCES

[1] Dowson, D., and Higginson, G. R., 1966, "*Elastohydrodynamic Lubrication*", Pergamon.

[2] Hamrock, B. J., and Dowson, D., 1981, "*Ball Bearing Lubrication*", John Wiley & Sons.

[3] Gohar, R., 1988, "*Elastohydrodynamics*", Ellis Horwood.

[4] LaBouff, G., and Booker, J. F., 1985, "*Dynamically Loaded Journal Bearings: A Finite Element Treatment for Rigid and Elastic Surfaces*", Transactions of the ASME Journal of Tribology, Vol. 107, pp. 505-515.

[5] Fantino, B., and Frene, J., 1985, "*Comparision of Dynamic Behaviour of Elastic Connecting-Rod Bearing in Both Petrol and Diesel Engines*", ASME Journal of Tribology, Vol. 107, pp. 87-91.

[6] Oh, K. P., and Goenka, P. K., 1985, "*The Elastohydrodynamic Solution of Journal Bearings Under Dynamic Loading "*, Transactions of the ASME Journal of Tribology, Vol. 107, pp. 389-395.

[7] van der Tempel, L., Moes, H., and Bosma, R., 1985, "*Starvation in Dynamically Loaded Flexible Short Journal Bearings",* Transactions of the ASME Journal of Tribology, Vol. 107, pp. 516-521.

[8] van der Tempel, L., Moes, H., and Bosma, R., 1985, "*Numerical Simulation of Dynamically Loaded Flexible Short Journal Bearings"*, Transactions of the ASME Journal of Tribology, Vol. 107, pp. 396-401.

[9] Kumar, A., Booker, J. F., and Goenka, P. K., 1990, "*Modal Analysis of Elastohydrodynamic Lubrication: A Connecting Rod Application"*, Transactions of the ASME Journal of Tribology, Vol. 112, pp. 524-534.

[10] Dursunkaya, Z., Keribar, R., and Ganapaty, V., 1994, " *A Model of Piston Secondary Motion and Elastohydrodynamic Skirt Lubrication"*, ASME Journal of Tribology, Vol. 116, pp. 777-785.

[11] Greenwood, I. A., and Tripp, J. H., 1971, "*The Contact of Two Nominally Flat Surfaces"*, Proc. IMechE, Vol. 185, pp. 625-633.